JCTC Journal of Chemical Theory and Computation

Density Functional Static Dipole Polarizability and First-Hyperpolarizability Calculations of Na_n ($n = 2, 4, 6, 8$) Clusters Using an Approximate CPKS Method and its Comparison with MP2 Calculations†

K. B. Sophy,‡ Patrizia Calaminici,§ and Sourav Pal*,‡

Theory Group, Physical Chemistry Division, National Chemical Laboratory, Pune 411 008, India, and Departmento de Quimica, CINVESTAV, Av. Instituto Politecnico Nacional 2508, A. P. 14-740 Mexico, D. F. 07000, Mexico

Received December 14, 2006

Abstract: We report the static dipole polarizability and first-hyperpolarizability of the sodium atom clusters, Na_n, $n = 2$, 4, 6 and 8, using our recent implementation of a numerical-analytical approach to the coupled-perturbed Kohn−Sham (CPKS) equations in deMon2k. The calculations are reported for VWN and BP86 exchange-correlation functionals using Sadlej and TZVP-FIP1 basis sets which have been previously optimized for polarizability calculations. All-electron calculations were performed for the optimizations at the VWN/DZVP/A2 and PW86/DZVP/A2 levels. Comparisons are made with Hartree−Fock (HF) and MP2 benchmark calculations.

Introduction

Linear and nonlinear response electric properties, namely, dipole polarizability and dipole first-hyperpolarizabilities, of metal clusters have been of considerable interest over the past decade.[1] The size dependence of the optical properties[2,3] makes the study of clusters even more interesting for understanding the correlation between the two. Clusters[3] are aggregates of atoms or molecules, generally intermediate in size. Clusters of up to 40 atoms are considered to be small sized. The properties of small clusters vary so much with size and shape that their correlation with number of component particles is not simple. For large clusters the properties approach those of the corresponding bulk material. Molecules are characterized by having definite compositions and, in most cases, definite structures. The properties of clusters, on the other hand, depend on the number of atoms in the cluster and so does the most stable structure. Clusters thus differ from conventional molecules because of composition and structure. Clusters could be composed of any number of particles of the same or different kind and can be further classified as homogeneous or heterogeneous clusters, respectively, and for most of them as the number of atoms increases, the number of stable structures grows rapidly. Clusters have drawn interest for several reasons. There are powerful ways to study them, both experimentally and theoretically. Clusters may give way to make altogether new kinds of materials, to carry out chemical reactions in new ways, and to gain understanding of the intermediate matter, which exist as one goes from molecules to crystals to bulk. All these makes cluster science a fascinating field, which not only enriches the fields around it but also offers tantalizing possibilities for new materials and processes.

Metal clusters, in general, have been studied to a reasonable extent.[4] However, the presence of a single valence electron makes the alkali metal clusters the simplest metal cluster, and, therefore, it has been used as a prototype system for understanding the size effects in metal clusters. Here, we would concentrate on sodium clusters of up to 8 atoms. Polarizabilities for the sodium clusters have been reported using theory[5−13,16] as well as experiments.[14−17] Guan et al. (ref 12 and references therein) have done all-electron density functional calculations for Na_n ($n = 1−6$) clusters using local and gradient-corrected functionals. They have discussed several popular models for studying polarizability of clusters

† Dedicated to Dennis R. Salahub on the occasion of his 60th birthday.

* Corresponding author fax: 91-20-25902636; e-mail: s.pal@ncl.res.in.

‡ National Chemical Laboratory.

§ CINVESTAV.

10.1021/ct6003627 CCC: $37.00
Published on Web 03/08/2007

spanning the simplest and oldest conducting sphere model for studying the clusters to the free electron model used for studying the bulk alkali metals. Guan et al. have also mentioned about the quantum mechanical jellium sphere approximation differing from the classical sphere model due to the fact that the quantum mechanical density extends beyond the radius of the classical sphere, thus the effective sphere being larger.

In this paper, we will study the correlation of response electric properties with size for the homonuclear alkali metal clusters of sodium using an approximate formalism proposed by us earlier.[18−20] We study the dipole polarizability and the first-hyperpolarizability of the even number of Na atom clusters using local density approximation (LDA) and generalized gradient approximation (GGA) based exchange-correlation functionals in the presence of an external homogeneous static electric field perturbation. We will also discuss the effect of electron correlation on the polarizabilities. We have done an all-electron calculation for the optimizations as well as for the response properties. Calculations, that consider all the electrons in the cluster, are not very common. This is especially the case for ab initio calculations. There are some all-electron optimizations available using the DFT.[12,13]

The paper is organized in the following manner. The theoretical methods used and the computational and technical details of our calculations are described in the following section. We will discuss our results in section 3 and summarize our conclusions in section 4. Unless otherwise stated, we use atomic units throughout this paper.

Theoretical Methods and Computational and Technical Details

A. Theory. DFT[21,22] has been widely used for molecular response property calculations. Response property of molecule is the response of the molecule to some kind of perturbation. For an external perturbation the molecular energy has a dependence on the perturbation and can be expanded as a Taylor series expansion. In the presence of a static electric field perturbation, the energy expansion becomes

$$E(F) = E(0) - \sum_i \mu_i F_i - \frac{1}{2}\sum_{i,j} \alpha_{ij} F_i F_j - \frac{1}{6}\sum_{i,j,k} \beta_{ijk} F_i F_j F_k - \ldots \quad (1)$$

where i, j, and k are summation indices each spanning the x, y, and z direction, the first term is the energy of the molecule in the absence of the electric field perturbation, F, the second term, gives the dipole moment, the third term gives the dipole polarizability, the fourth term gives the dipole first-hyperpolarizability, and so on ....

Alternatively, the field dependent dipole moment in turn can be written as

$$\mu_i(F) = \mu_i + \sum_j \alpha_{ij} F_j + \frac{1}{2}\sum_{j,k} \beta_{ijk} F_j F_k + \ldots \quad (2)$$

where i, j, and k are the x, y, and z directions, μ_i, α_{ij}, and β_{ijk} are the component of the permanent dipole moment, dipole polarizability, and the dipole first-hyperpolarizability, respectively, and so on .....

These molecular electric response properties can be obtained by explicitly obtaining the derivatives of energy with respect to the perturbation, i.e., analytically using the coupled Kohn−Sham method[23−28] or by doing a least-squares fit to a polynomial,[29] or by using a numerical finite-field method. Choosing the finite field values symmetrically (e.g. 0.001 au, like we have chosen in this work), the next highest contamination in the numerical procedure can be eliminated, thus ensuring more numerical stability of the results. However, the precision in the calculation of energies limits the size of the field value. In the analytical response approach, the CPKS equations need to be solved to obtain the response of the electron density in terms of the derivative of the molecular orbital coefficients. The CPKS matrix equations are basically the derivative of the perturbed KS operator matrix equations with respect to the electric field perturbation, which means that the Hamiltonian has a dependence on the electric field and can be written as

$$H(F) = H_0 + \mu F \quad (3)$$

where the first term is the unperturbed Hamiltonian, and the second term is the perturbation that is linear in field, F. We thus have a linear response term in the Hamiltonian. Solving the CPKS equations, we can obtain the perturbed density matrix. And, due to the variational nature of the DFT we can make use of the $(2n+1)$ rule for the energy derivative[30] which is a result of the Hellmann−Feynman theorem.[31,32] As a consequence, the first-order response of the electron density which is the first-order change in the density can be used to obtain response properties up to the third order. This means that we can evaluate not only the dipole polarizability but also the dipole first-hyperpolarizability using this response of the electron density.

B. Computational and Technical Details. The linear combination of the Gaussian-type orbitals Kohn−Sham density functional theory (LCGTO-KS-DFT) method, as implemented in the program deMon2k,[33] was used to carry out all geometry optimizations and harmonic vibrational frequency calculations. The program uses the formalism of the Kohn−Sham equations[34] and analytic energy gradients for the structure optimizations. The exchange-correlation potential was numerically integrated on an adaptive grid.[35] The grid accuracy was set to 10^{-5} in all calculations. The Coulomb energy was calculated by the variational fitting procedure proposed by Dunlap, Connolly, and Sabin.[36,37] For the fitting of the density, the *AUXIS* option with the auxiliary function set A2[38] was used in all the optimization calculations and the vibrational analysis calculation following the previous work of Calaminici et al.,[13] which was found sufficient for the purpose. In order to localize different minima on the potential energy surface (PES), the structures of the studied sodium clusters have been optimized considering as starting points different initial geometries and multiplicities. In order to avoid spin contamination the calculations were performed with the restricted open shell Kohn−Sham (ROKS) method. The ROKS method in deMon2k is the DFT analog of the Roothaan's open shell equations for HF theory; it means that

all coupled alpha and beta electrons occupy the same space orbital and that the corresponding close shell exchange-correlation potential is given as an average of the alpha and beta exchange-correlation potential. The calculations were performed in the LDA using the exchange-correlation contributions proposed by Vosko, Wilk, and Nusair[39] and employing all-electron basis sets.[38] The same functional was used for the frequency analysis in order to distinguish between minima and transition state on the potential energy surface (PES). Cluster optimizations were also carried out at the GGA using the same basis and auxiliary function set with the exchange-correlation functional of Perdew and Wang (PW86).[40,41] A quasi-Newton method in internal redundant coordinates with analytic energy gradients was used for the structure optimization.[42] The convergence was based on the Cartesian gradient and displacement vectors with a threshold of 10^{-4} and 10^{-3} au, respectively. For the sodium tetramer, the GGA calculation required tougher convergence criteria of 10^{-7} and 10^{-6} due to the fact that at this level of theory the PES of this system is extremely flat. A vibrational analysis was performed in order to discriminate between minima and transition states. The second derivatives were calculated by numerical differentiation (two-point finite difference) of the analytic energy gradients using a displacement of 0.001 au from the optimized geometry for all 3N coordinates. The harmonic frequencies were obtained by diagonalizing the mass-weighted Cartesian force constant matrix. The response property calculations were then freshly carried out for these ground-state Na cluster geometries.

We have used the 1.7 version[43] of deMon2k, in which we have incorporated a numerical-analytical CPKS method (a simplified approximation), earlier proposed by us.[18−20] We use the POLAR keyword in the deMon2k program, which employs a finite field approximation to obtain dipole-based polarizabilities of molecules. This option in deMon2k leads to a series of calculations involving different electric field perturbations (namely, −0.001 and 0.001, in atomic units) to the Hamiltonian around zero field value. Using these, we construct the derivative KS-operator matrix in the finite field approximation. The choice of the field strengths at an interval of 0.001 au could be justified by simply noting the difference between the calculated β value and the theoretical value of zero for Na_2. We have used the field value of 0.001 au in our response calculations as the error in our β value of Na_2 was minimum for this interval, the error increased for any value around 0.001 au. A separate module has been introduced by us, into the deMon2k for carrying out the CPKS procedure so as to obtain the response of the electron density in terms of the perturbed coefficient matrix. The CPKS equation to be solved for obtaining the response of the coefficient matrix is

$$U'_{ia} = \frac{\sum_{\mu,\nu} C^{\dagger}_{\mu i} H'_{\mu\nu} C_{\nu a}}{(\epsilon_i - \epsilon_a)} \tag{4}$$

where the C and the ϵ are the coefficient matrix and the eigenvalues of the unperturbed DFT calculation. H' is the derivative KS-operator matrix (which in principle needs to be constructed analytically for every iteration) constructed using the finite-difference 3-point formula for the first derivative just once for every direction. The U' matrix is related to the derivative coefficient matrix, C', which we are interested in through the unperturbed coefficient matrix, C, as

$$C' = CU' \tag{5}$$

The CPKS module is thus used to obtain a single-step solution of the CPKS equations for each of the three, *x*, *y*, and *z*, directions by using our method of approximating the derivative KS-operator matrix for each direction and plugging in the equation for U' to obtain the respective derivative coefficient matrices. These are then used to obtain the derivative density matrices which are the response of the electron density in the three directions. We thus have three derivative density matrices. The polarizability is obtained as the trace of the product of the derivative density matrix for a direction *a* with the dipole moment integrals in direction *b*, where *a* and *b* span the *x*, *y*, and *z* directions, thus giving the corresponding polarizability component. Thus all the components of the polarizability tensor can be obtained using the derivative density matrix. The first hyperpolarizability which is the third derivative of energy with respect to the electric field can also be obtained as per the $(2n+1)$ rule.[30] The first-hyperpolarizability can be trivially obtained using the derivative KS-operator matrix in the MO basis and derivative coefficient matrix for all permutations thus obtaining each of the components of the hyperpolarizability tensor. The novelty of our method lies in the simple single-step solution to the CPKS equations which avoids the complicated algebra as well as expensive computational time that would be required to construct the analytic derivative KS-operator matrix involving the derivative of the exchange-correlation term. Also the derivative KS-operator matrix needs to be evaluated for every iteration. Our method circumvents this complication thus saving time and computational effort. It is highly advantageous for response property calculations involving large molecules or large basis sets or both.

We report the mean and anisotropic polarizability and mean first-hyperpolarizability values obtained using the respective tensor components. The mean polarizability was calculated from the polarizability components as

$$\bar{\alpha} = \frac{1}{3}(\alpha_{xx} + \alpha_{yy} + \alpha_{zz}) \tag{6}$$

and the polarizability anisotropy as

$$|\Delta\alpha|^2 = \frac{3\mathrm{tr}\alpha^2 - (\mathrm{tr}\,\alpha)^2}{2} \quad \text{(general axes)} \tag{7}$$

$$= \frac{1}{2}[(\alpha_{xx} - \alpha_{yy})^2 + (\alpha_{xx} - \alpha_{zz})^2 + (\alpha_{yy} - \alpha_{zz})^2] \quad \text{(principal axes)} \tag{8}$$

The orientationally averaged first-hyperpolarizability were obtained as

$$\beta_i = \frac{1}{3}\sum_k \beta_{ikk} \tag{9}$$

$$\beta = \sqrt{\beta_x^2 + \beta_y^2 + \beta_z^2} \quad (10)$$

It is well-known that a general characteristic required for basis sets to perform well for polarizability calculation is that they should contain diffuse functions.[44] An economical strategy for constructing these kinds of basis sets is to augment valence basis sets of reasonable good quality with additional polarization functions.[45−48] We have chosen as valence basis a newly developed triple-ζ basis set (TZVP) which was optimized for gradient corrected DFT calculations.[49] The basis set was then augmented with three field-induced polarization (FIP) functions, two p and one d, which were derived following the work of Zeiss et al.[46] They derived the FIP function exponents from an analytic analysis of the field-induced charges in hydrogen orbitals. The exponents of the additional FIP functions have been presented already in ref 13. In order to avoid the contamination of the valence basis set with the diffuse p- and d-type Gaussians of the FIP functions, spherical basis functions are used in all the calculations. We have named the resulting basis set TZVP-FIP1. Our DFT response property calculations were done using the Sadlej[45] and TZVP-FIP1 basis sets with the *CARTESIAN* option for the orbitals. We did not employ the auxiliary basis for fitting the exchange-correlation functional in our response property calculations; i.e. the *VXCTYPE BASIS* option was used. The calculations were done using the LDA based VWN[39] and GGA based BP86[50,41] functionals in the deMon2k for both the basis sets. This entire set of response calculations was repeated for both sets of Na cluster geometries. In our calculations we have chosen only closed shell Na clusters due to the fact that we have implemented the linear response approach in a numerical-analytical manner in the deMon2k only for closed shell cases. We have therefore used the restricted Kohn−Sham (RKS) scheme of calculation, where the grid accuracy of 10^{-6} au was used for the property calculations. The density convergence was set to 10^{-10} au in the HF and MP2 as well as DFT calculations. The HF and MP2 benchmark calculations were carried out using the GAMESS,[51] and the DFT calculations were done using deMon2k program. The DFT optimized structures were used for the MP2 and the HF calculations. These properties are evaluated using the finite field method available in GAMESS for a finite field value of 0.001 au. The results are discussed in the following section.

Results and Discussion

A. Equilibrium Geometries. We report the ground-state structures of the even number of sodium atom clusters from dimer to octamer obtained using the VWN and PW86 (bond distances in parenthesis) functionals in Figure 1. The equilibrium structures obtained from both functionals are similar and show a general topological agreement with the earlier theoretical reports.[6,7,52] All-electron type optimizations for the sodium clusters using GGA based functionals are available but scarce.[12,13] We have carried out all-electron type optimization for both VWN as well as PW86 functionals in the present work.

The dimer bond distance is equal to 3.017 Å with both the optimizations, whereas the experimental value is 3.078 Å.[53] The geometries for the remaining clusters differ very slightly for the two optimizations. The ground-state structure of Na_4 is a D_{2h} rhombic structure, whereas the one for the Na_6 is a C_{5v} pentagonal pyramid. The equilibrium geometry for the Na_8 is a rather compact dicapped octahedral (DCO) structure.

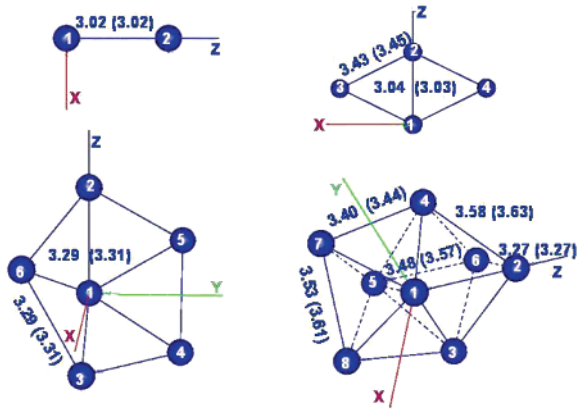

Figure 1. Calculated equilibrium geometries and the orientations used for the calculations of Na_n (n = 2, 4, 6, and 8) clusters using the VWN and PW86 (in parentheses) functionals and A2/DZVP basis. Bond distances in Å.

Table 1. Harmonic Frequencies (in cm^{-1}) for the Normal Modes of Na_n (n = 2, 4, 6, and 8) Clusters in Their Calculated Ground States Using VWN Functional and PW86 Functional with DZVP Basis Set and A2 Auxiliary Basis

cluster	VWN	PW86	expt
Na_2	161	160	159[a]
Na_4	35, 37, 77, 98, 144, 162	6, 43, 76, 100, 141, 163	
Na_6	31, 31, 55, 75, 77, 91, 91, 102, 102, 142, 147, 147	36, 36, 46, 70, 72, 89, 89, 93, 94, 140, 141, 142	
Na_8	32, 49, 56, 60, 65, 68, 73, 77, 85, 96, 108, 114, 119, 129, 134, 137, 141, 180	31, 49, 50, 57, 60, 64, 68, 69, 72, 74, 101, 101, 106, 121, 127, 130, 130, 131	

[a] From ref 54.

B. Harmonic Frequencies. We have tabulated the normal modes for both sets of optimized structures of the Na clusters in Table 1. The absence of imaginary frequency was used to confirm that all the optimized structures were minima on the PES. The reported experimental frequency for the dimer is 159 cm^{-1}.[54] Our calculation for dimer using the VWN and PW86 functionals gave 161 and 160 cm^{-1} values, respectively, which are in good agreement with the experimental value. Earlier calculations of tetramer harmonic frequencies by Dahlseid et al.[55] at the configuration interaction-singles (CIS) level gave 27, 43, 73, 98, 130, and 150 as the frequencies. The qualitative trend for our harmonic frequencies in Table 1 is similar, except for the first frequency for the tetramer at the PW86 level which is small. It can be seen that the first few frequencies of the clusters are smaller in magnitude. This could be attributed to the extremely flat PES of the clusters which further complicates the distinction between the global and the local minima. This

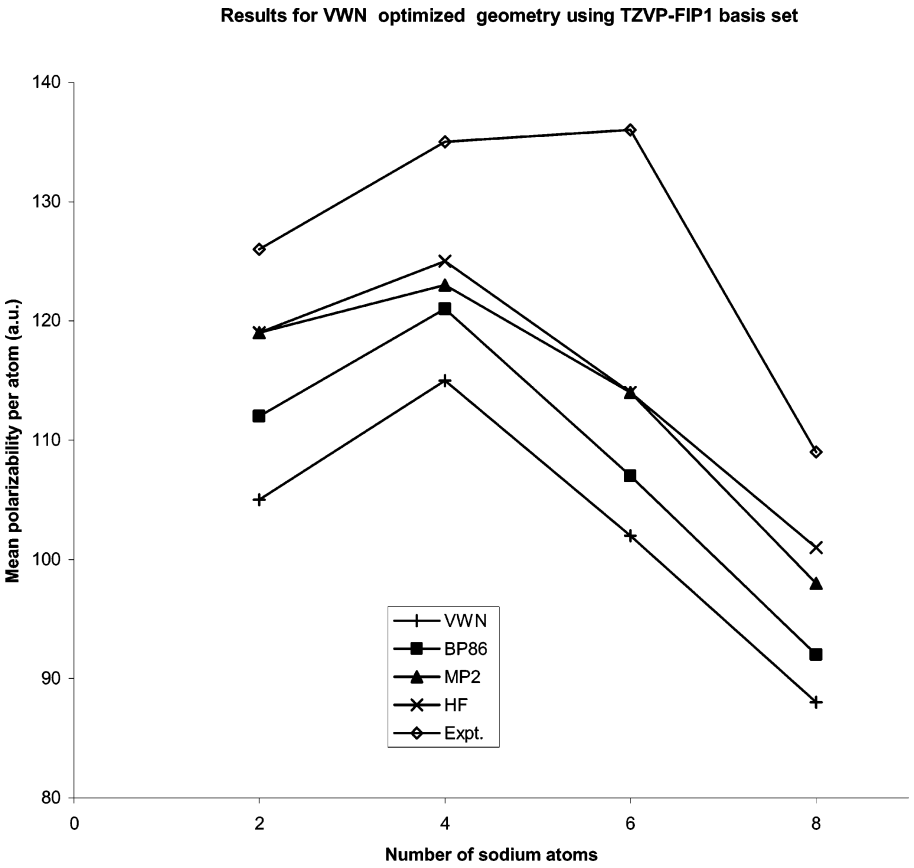

Figure 2. A plot of calculated mean polarizability per atom using the TZVP-FIP1 basis for Na_n (n = 2, 4, 6, and 8) clusters optimized using VWN/A2/DZVP versus number of atoms.

could especially be a serious problem as we go to even larger clusters where the number of stable configurations increases drastically. In our calculations we had to tighten the convergence criterion for the tetramer due to its flat PES to obtain a minimum energy structure.

C. Static Mean Polarizability, Polarizability Anisotropy, and First-Hyperpolarizability. We have calculated the mean polarizability, $\bar{\alpha}$, and polarizability anisotropies, $|\Delta\alpha|$, for the optimized minimum energy structures of Na_2, Na_4, Na_6, and Na_8, which are even numbered sodium atom clusters. We have also done the calculations for the dipole first-hyperpolarizability. Our calculations have been carried out at the DFT level. MP2 level calculations were done for benchmarking our results. We also carried out calculations at the HF level to put correlation effects in a clearer perspective. Additionally, we have also collected the dipole-based finite field polarizabilities as available in the deMon2k program to compare with our DFT polarizability values. The results are presented in graphical as well as tabular form. The graphs contain plots of mean polarizability per atom in atomic units against the number of atoms and compared with the available experimental values. The experimental values were calculated from the measurement of relative polarizabilities of Knight et al.[14] and the absolute measurement of the atomic polarizability by Molof et al.[17] We will first discuss the polarizability results presented graphically. The DFT response property calculations have been done using the VWN and BP86 functionals. The basis sets used for the calculations are Sadlej and TZVP-FIP1. There are two sets of Na cluster geometries used for the calculations, one optimized using a VWN functional and the other optimized using the PW86 functional, and both sets are optimized using the DZVP/A2 basis set. Each figure has a plot showing the mean polarizability per atom, ($\bar{\alpha}/n$); values for all four Na clusters obtained at the VWN, BP86, MP2, and HF level of theory were compared with the experimental values. These are presented in Figures 2−5 corresponding to the combination of the exchange-correlation functional used for the optimization and the basis set used for the polarizability calculation. Comparison of the DFT values from the plots for the two sets of geometries shows that for a given basis set and exchange-correlation functional the results do not show any change except for 1−2 au, which means that the level of optimization of the geometries do not affect the mean polarizability per atom for the DFT calculations. Since the trends for the mean polarizability per atom are similar for both sets of optimized geometries of Na clusters, we will discuss only the general trend pointing out any difference wherever necessary.

A particular trend that can be seen for the mean polarizability per atom values for the VWN, BP86, MP2, and HF calculations in all the plots is that the values from the theoretical calculations for all the Na clusters are less than the experimental values of the mean polarizability per atom, except at two places for the calculations using the Sadlej basis set, one, in Figure 5 for both the HF as well as MP2 values of the Na_2 cluster optimized at the PW86 level and second, in Figure 3 for the MP2 value for the VWN

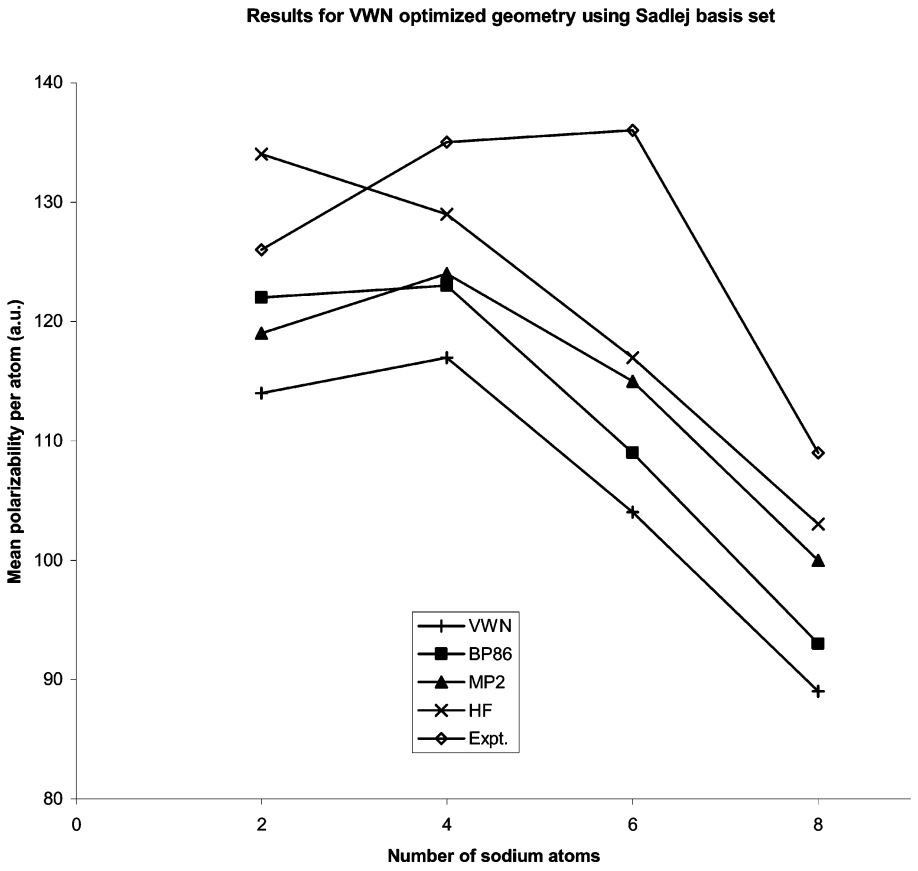

Figure 3. A plot of calculated mean polarizability per atom using the Sadlej basis for Na_n ($n = 2$, 4, 6, and 8) clusters optimized using VWN/A2/DZVP versus number of atoms.

optimized Na_2 cluster. The value for the Na_2 cluster in both cases is overestimated from that of the experiment by 8 au which is about 6% as seen in both Figures 3 and 5. Also, the values from MP2 and the HF are closest to the experimental values followed by the ones using GGA BP86, the exception being in the case of calculations done using the Sadlej basis for the Na_2 cluster optimized using the VWN functional where the BP86 values are closer to experiment as is evident from Figure 3. The VWN values, in general, show the largest deviation from the experimental values. This is in line with the correlation effects being incorporated in the exchange-correlation functionals used for the DFT and the MP2 theory. For VWN which is a LDA based functional, the density is mapped locally to a homogeneous electron gas picture which exhibits a strong overestimation of the correlation effects as is well-known. However, for the mapping of the response of the density as a consequence of the external electric field perturbation, the VWN functional is unable to show that strong correlation effects which are probably due to less nonlocal effects in the density redistribution. This can be clearly seen in the values of mean polarizability per atom which are farthest from the experimental ones in Figures 2−5. The BP86 nonlocal functional and the ab initio methods, on the other hand, show the nonlocality in the density response although to different extents thus giving relatively higher values in comparison to VWN ones in all the plots. If we observe the trend in the experimental values of the Na clusters, we see that the polarizability per atom values increases from Na_2 to Na_4 to a reasonable extent, then there is a very slight increase from Na_4 to Na_6, whereas from Na_6 to Na_8 there is a drastic drop in the value. Qualitatively this trend is more correctly reflected by all four methods for the values from the TZVP-FIP1 basis for both sets of geometries. For the Sadlej basis however, both the HF and MP2 values overshoot the experimental value of 126 au as seen in Figure 5 for the Na_2 cluster optimized at the PW86 level; similarly Figure 3 shows an overestimation of the HF polarizability value for the Na_2 cluster optimized at the VWN level. Also the slight increase in experimental value from Na_4 to Na_6 is seen to be otherwise in all the calculations, independent of the optimization and level of calculation. The maximum deviation from the experimental values is for the Na_6 cluster results, irrespective of the level of theory used. This is the case for every calculation, the highest being 25% for the VWN method in Figure 2. A comparison of the similarity in the plots for the TZVP-FIP1 basis set (i.e., Figures 2 and 4) and the Sadlej basis set (i.e., Figures 3 and 5) for the two sets of optimized geometries show that the level of optimization does not affect the polarizability calculations at the DFT level. This similarity in the plots can also be seen for the MP2 calculations using the TZVP-FIP1 basis set (i.e., Figures 2 and 4); however, this is not the case for the Sadlej basis (Figures 3 and 5). The behavior of the MP2 as well as HF calculations for the two basis sets could be assigned to the fact that the TZVP-FIP1 basis set has been optimized for the polarizability calculation using DFT, whereas the Sadlej basis is an optimized basis for the polarizability calculation using ab initio methods.

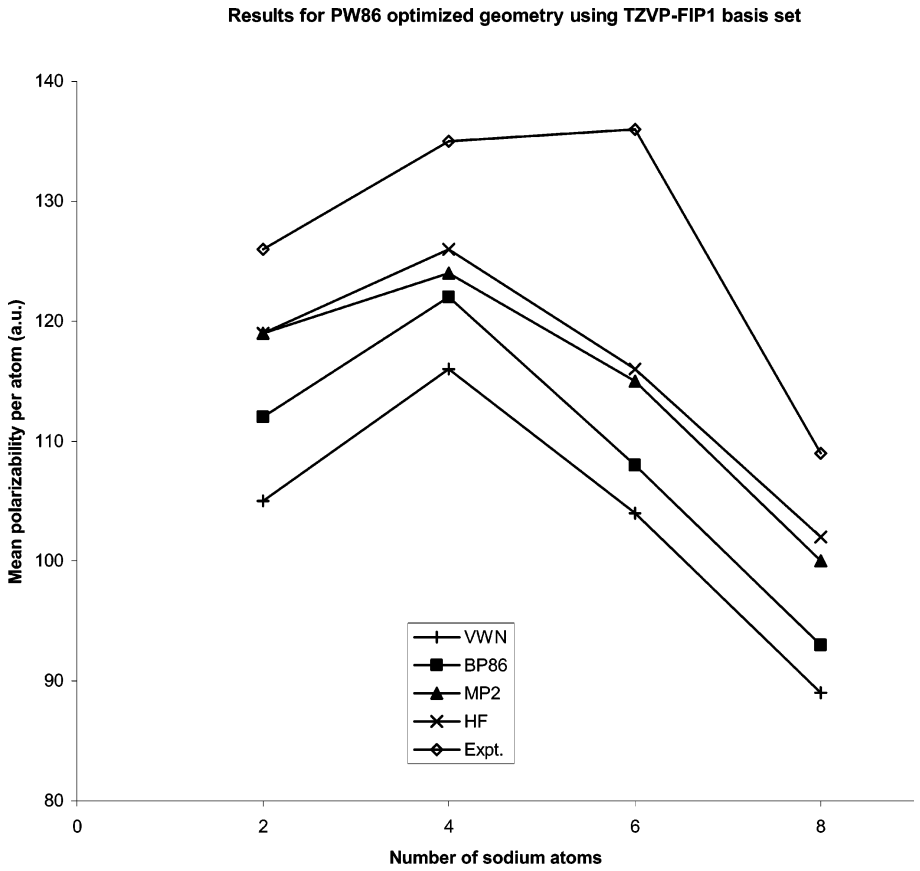

Figure 4. A plot of calculated mean polarizability per atom using the TZVP-FIP1 basis for Na_n (n = 2, 4, 6, and 8) clusters optimized using PW86/A2/DZVP versus number of atoms.

In Table 2, we have compared the experimental and DFT mean polarizability per atom values obtained by Rayane et al.[16] in angstrom units with our DFT calculations for the Na cluster geometries optimized at the PW86-DZVP-A2 level. We have compared our results for the VWN and BP86 functionals obtained using the Sadlej and TZVP-FIP1 basis sets. The comparison has been done with the values reported by Rayane et al.[16] calculated at the PW91 level for the SU and 6-31G basis sets and measured experimentally. Although we have discussed our mean polarizability per atom values above earlier, we would like to have a comparison with other DFT results available. It can be clearly seen that the values reported by Rayane et al. are closer to the experiment as compared to our results. They have argued that the SU basis gives values closer to the experiment in comparison with the 6-31G basis as there is more polarization (d-orbitals) and diffuse functions in the SU basis which are expected to be important for polarizability calculation. On a similar basis, we could assign the marginally better behavior of the Sadlej basis as compared to the TZVP-FIP1 basis, especially for the dimer, to the fact that there is a larger number of polarization functions in the Sadlej basis as compared to the TZVP-FIP1, whereas there are more diffuse functions in the TZVP-FIP1 basis set. Another reason for TZVP-FIP1 not performing better than the Sadlej basis despite being optimized for DFT could be the use of Cartesian basis functions in all our response property calculations. The use of spherical basis functions is advised to avoid contamination of the valence basis set with the diffuse p- and d-type Gaussians of the FIP functions. This could be explained by taking an example of s- and d-orbitals located on the same center. In the spherical representation of these two orbitals shells, i.e., the orbitals are constructed from a one-dimensional radial function and real spherical harmonics, the overlap matrix elements vanish due to the orthogonality of the spherical harmonics, whereas in the case of Cartesian representation the d shell is overdetermined by a total symmetric component ($d_{xx} + d_{yy} + d_{zz}$) that can mix with the s-orbitals (a similar situation holds for the p- and f-shells). Rayane et al.[16] have also concluded that diffuse functions are less important for static response in the ground-state calculations of clusters. Calculated values of polarizability per atom using the PW91 functional reported by Rayane et al. are in better agreement with the experiments than our values calculated using VWN and BP86. In our calculation we find that the values obtained from the BP86 are closer to the experiment than the VWN ones.

Tables 3−6 present our calculations done for each of the Na clusters, i.e., each cluster calculations are presented in separate tables. We have reported the polarizability anisotropy and the orientationally averaged first hyperpolarizability values obtained using the DFT, HF and MP2 calculations in these tables. The DFT finite field (FF) results of polarizability are also presented in the tables for comparison. We have already discussed the mean polarizability per atom values presented in Figures 2−5. We now turn to the mean polarizability values and the polarizability anisotropy values given in Tables 3−6. As we move across Tables 3−6 for

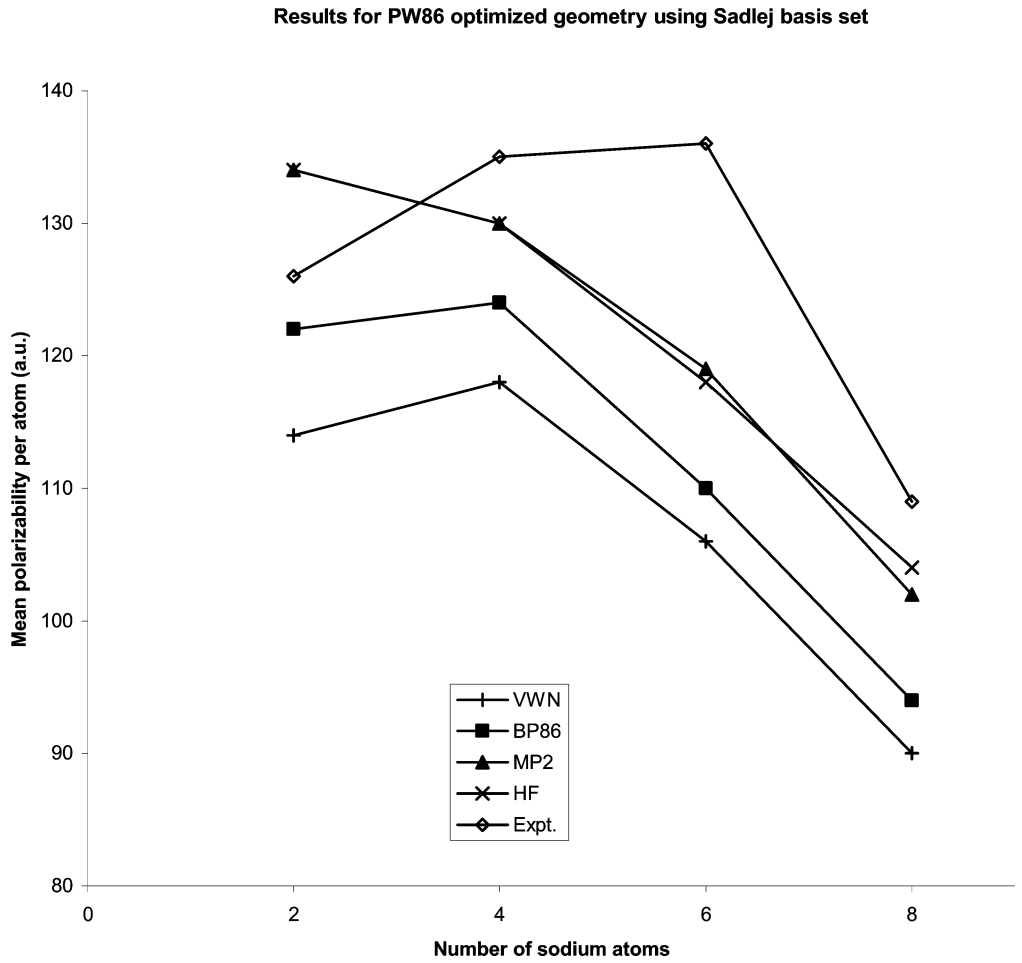

Figure 5. A plot of calculated mean polarizability per atom using the Sadlej basis for Na_n ($n = 2$, 4, 6, and 8) clusters optimized using PW86/A2/DZVP versus number of atoms.

the clusters Na_2 through Na_8, we observe that the DFT polarizability anisotropy value increases as we move from the dimer to the tetramer and decreases as we go to the hexamer and octamer. This trend in the values reflects the clear relation between the cluster structure and the polarizability anisotropy values. It is worth noting that as the cluster structure becomes compact like in the case of the octamer the polarizability anisotropy value decreases. The value for the octamer is even less than the value for the dimer which has an open structure. As we go from the tetramer to hexamer, we see that the hexamer being a closed structure as against the planar tetramer, it shows a decrease in the polarizability anisotropy value from that of the tetramer. A comparison of the polarizability anisotropy values for all the clusters among the two basis sets for each of the methods shows that the Sadlej basis gives values lesser than the TZVP-FIP1 basis, except for the case of the hexamer where the trend is reversed. A general trend of the BP86 functional giving slightly higher values for the polarizability anisotropy than the VWN functional can be seen in all the calculations. We could not compare our results with experiments as there is no experimental measurement of polarizability anisotropy available.

The implications from the values of the mean polarizability for the different methods, basis sets, and functionals used would now be discussed. The TZVP-FIP1 basis used in the

Table 2. Calculated Values of Static Mean Polarizabilities per Atom (in Å^3) for Na_n Clusters ($n = 2$, 4, 6, and 8) Optimized at the PW86/DZVP/A2 Level in Comparison with Theory and Experiment

clusters	XC	basis	$\bar{\alpha}/n$
Na_2	PW91	SU[a]	19.1
	PW91	6-31G[a]	19.0
	VWN	Sadlej (TZVP-FIP1)	16.9 (15.5)
	BP86	Sadlej (TZVP-FIP1)	18.0 (16.6)
		expt[a]	19.65
Na_4	PW91	SU[a]	19.6
(rhombus)	PW91	6-31G[a]	19.3
	VWN	Sadlej (TZVP-FIP1)	17.5 (17.2)
	BP86	Sadlej (TZVP-FIP1)	18.4 (18.0)
		expt[a]	20.95
Na_6	PW91	SU[a]	17.4
(pentagonal	PW91	6-31G[a]	17.3
pyramid)	VWN	Sadlej (TZVP-FIP1)	15.6 (15.4)
	BP86	Sadlej (TZVP-FIP1)	16.3 (16.1)
		expt[a]	18.63
Na_8	PW91	SU[a]	14.9
(DCO)	PW91	6-31G[a]	14.6
	VWN	Sadlej (TZVP-FIP1)	13.3 (13.3)
	BP86	Sadlej (TZVP-FIP1)	13.9 (13.8)
		expt[a]	16.69

[a] From ref 16.

Table 3. Static Mean Polarizability, Polarizability Anisotropy, and Mean First-Hyperpolarizability of Na_2 Cluster Optimized with DZVP/A2 (in Atomic Units)

optimized	basis set	method	$\bar{\alpha}$	$\lvert\Delta\alpha\rvert$	$\beta_x = \beta_y$	β_z	β
VWN	TZVP-FIP1	MP2	237.08		0.0	0.0	0.0
		VWN	209.48	157.17	0.0	1.0	1.0
		VWN-FF	209.41	157.47			
		BP86	223.96	169.23	0.0	1.7	1.7
		BP86-FF	223.63	170.17			
		HF	237.37		0.0	0.0	0.0
	Sadlej	MP2	268.69		0.0	0.0	0.0
		VWN	227.98	132.07	0.0	1.6	1.6
		VWN-FF	227.89	132.60			
		BP86	243.02	140.96	0.0	2.5	2.5
		BP86-FF	242.66	142.31			
		HF	267.12		0.0	0.0	0.0
PW86	TZVP-FIP1	MP2	237.08		0.0	0.0	0.0
		VWN	209.48	157.17	0.0	1.0	1.0
		VWN-FF	209.41	157.47			
		BP86	223.96	169.23	0.0	1.7	1.7
		BP86-FF	223.63	170.17			
		HF	237.37		0.0	0.0	0.0
	Sadlej	MP2	268.69		0.0	0.0	0.0
		VWN	227.98	132.07	0.0	1.6	1.6
		VWN-FF	227.89	132.60			
		BP86	243.02	140.96	0.0	2.5	2.5
		BP86-FF	242.66	142.31			
		HF	267.12		0.0	0.0	0.0
expt			251.90				

[a] Experimental values calculated from the measurement of relative polarizabilities of Knight et al.[14] and the absolute measurement of the atomic polarizability by Molof et al.[17]

response property calculations is optimized for the gradient-corrected functions and is not correlation consistent. Although is may be too small for ab initio MP2 calculations, we have carried out the MP2 calculations using the TZVP-FIP1 basis set for benchmarking our results. On the other hand, the Sadlej basis is optimized for ab initio polarizability calculations and is a medium-sized basis as compared to the TZVP-FIP1. As the number of atoms in the cluster increases the mean polarizability value increases. Our DFT mean polarizability values deviate from the corresponding finite-field DFT mean polarizabilities by less than 0.4 au for the dimer, 0.6 au for the tetramer, 1.6 au for the hexamer, and by less than 2.8 au for the octamer. Also, the mean polarizability values from the GGA based BP86 functional are closer to the experimental values as compared to the ones using the VWN functional, for both sets of optimized sodium clusters. All this can be clearly observed from the mean polarizability values of the clusters in Tables 3−6.

The following critical observations are made after comparison of the DFT mean polarizability values with the MP2 and HF values. In general, both the HF and the MP2 mean polarizability values are closer to the experimental values as compared to the DFT results. In fact, certain HF values are closer to the experimental results than the MP2 values which is unexpected, as MP2 is a correlated method, whereas HF theory lacks correlation terms in its energy expression. Also, usually DFT is believed to perform better than the HF theory due to incorporation of the correlation effects. We, however, see that as we go from the TZVP-FIP1 basis to the Sadlej in each of the tables (Tables 3−6), the mean polarizability value increases for the DFT and HF as well as the MP2 method. But what is worth noting is that the HF overshoots the experimental value for the dimer in Table 3 for the Sadlej basis. This can be used to understand the basic problem in the HF theory that as the basis set size increases further the mean polarizability value would go way beyond the experimental value. The results from MP2 theory do not show much improvement either, since MP2 energy does not contain contributions from a singly excited determinant, which are important for dipole based properties. The improvement may start appearing only at the MP4 level. However, MP4 calculations are computationally very expensive. It could be observed that although the DFT values are not closer to the experiments there is a significant increase as we go from the TZVP-FIP1 basis to the Sadlej and as we move from a local to a nonlocal functional. As a consequence, we could expect the mean polarizability values to approach the experimental values as the basis set size increases. The correlation effects due to a proper choice of the exchange-correlation functional may improve the results further. Thus it can be seen that for the response property calculation DFT provides a better choice than even the MP2 ab initio method. It may be noted that the temperature effects which are present in the experiments is missing in the above theories, which makes the comparison of theory with experiment difficult.

We now discuss the hyperpolarizability values from our calculations. Due to the absence of experimental data, we compare the DFT calculations with our HF and MP2 results. The β value for the dimer should be zero; however, we see that in Table 3 there is a negligible value of at most 2.5 au for the DFT calculations. This error shoots up for selections of the electric field strengths other than 0.001 au which was chosen for these calculations. The error for the β values of the dimer could be assigned to the percolation of the inaccuracies into the response density matrix due to the numerical approximation employed for obtaining the derivative KS-operator matrix in our method. For the tetramer in Table 4 the β_x values for the VWN optimized structure varies between 14 and 20 au which is reflected in the β as the components along the other two directions are relatively lesser in magnitude for the Sadlej and the TZVP-FIP1 basis, whereas the β values for the PW86 optimized geometry are close to zero. The β value for the TZVP basis from the BP86 method is closer to the MP2 value of 21.3 au, whereas for the Sadlej basis the β value for the VWN is closer to the corresponding MP2 value of 14.1 au and the value for the BP86 is overestimated for the VWN optimized structure. The HF β values are less than the MP2 and corresponding DFT values. As we move to the PW86 optimized structure results in Table 4, the β values from all methods are negligible. It can be seen that the tetramer has a rhombic planar structure that is symmetric due to which the β values are not very high. The β values are expected to increase as the asymmetry in the structure increases. The dimer and tetramer structures are nearly symmetric which is also reflected from the β values in the tables. As we move from tetramer to hexamer

Table 4. Static Mean Polarizability, Polarizability Anisotropy, and Mean First-Hyperpolarizability of Na_4 Cluster Optimized with DZVP/A2 (in Atomic Units)

optimized	basis set	method	$\bar{\alpha}$	$\|\Delta\alpha\|$	β_x	β_y	β_z	β
VWN	TZVP-FIP1	MP2	490.55		18.8	−1.8	−9.8	21.3
		VWN	459.58	452.84	15.6	−1.2	−9.2	18.2
		VWN-FF	459.42	454.36				
		BP86	482.30	472.29	19.7	6.5	−0.1	20.8
		BP86-FF	481.74	474.52				
		HF	498.39		6.9	−2.0	−7.3	10.2
	Sadlej	MP2	513.92		13.9	−1.4	2.0	14.1
		VWN	469.14	450.20	14.2	2.5	−3.0	14.7
		VWN-FF	469.18	452.38				
		BP86	492.84	468.94	16.6	5.4	−8.2	19.3
		BP86-FF	492.49	472.34				
		HF	515.55		0.3	−1.7	6.4	6.6
PW86	TZVP-FIP1	MP2	494.73		0.0	0.6	0.3	0.7
		VWN	463.43	463.43	0.0	−0.9	0.0	0.9
		VWN-FF	463.33	463.94				
		BP86	486.36	484.22	0.0	−1.2	0.1	1.2
		BP86-FF	485.81	484.48				
		HF	502.04		0.0	−0.6	0.0	0.6
	Sadlej	MP2	518.00		0.0	−0.5	0.1	0.5
		VWN	473.06	458.97	−1.5	−3.2	0.5	3.6
		VWN-FF	473.14	461.23				
		BP86	496.78	478.20	0.0	−0.8	0.1	0.8
		BP86-FF	496.52	481.58				
		HF	519.06		0.0	−0.4	0.0	0.4
expt			538.62					

[a] Experimental values calculated from the measurement of relative polarizabilities of Knight et al.[14] and the absolute measurement of the atomic polarizability by Molof et al.[17]

Table 5. Static Mean Polarizability, Polarizability Anisotropy, and Mean First-Hyperpolarizability of Na_6 Cluster Optimized with DZVP/A2 (in Atomic Units)

optimized	basis set	method	$\bar{\alpha}$	$\|\Delta\alpha\|$	β_x	β_y	β_z	β
VWN	TZVP-FIP1	MP2	680.80		−1266.9	−938.4	−773.0	1755.9
		VWN	614.16	374.13	−1621.4	−1200.5	−929.3	2221.2
		VWN-FF	613.87	374.35				
		BP86	640.91	390.11	−2046.4	−1478.9	−1207.3	2798.7
		BP86-FF	639.81	391.03				
		HF	683.24		−1173.7	−869.3	−712.8	1625.2
	Sadlej	MP2	704.06		−1147.9	−854.0	−705.9	1595.4
		VWN	623.65	377.87	−1332.2	−995.6	−819.1	1853.9
		VWN-FF	623.16	377.56				
		BP86	652.04	395.27	−1527.2	−1015.1	−798.6	2000.1
		BP86-FF	650.57	396.02				
		HF	701.13		−1172.3	−873.9	−719.3	1629.5
PW86	TZVP-FIP1	MP2	690.85		−1284.2	−983.7	−753.3	1784.5
		VWN	623.61	384.59	−1628.6	−1278.4	−832.6	2231.6
		VWN-FF	623.20	385.70				
		BP86	650.54	398.93	−2095.9	−1540.6	−1186.7	2859.1
		BP86-FF	649.66	401.80				
		HF	692.82		−1176.9	−901.1	−690.0	1635.0
	Sadlej	MP2	714.07		−1157.4	−888.9	−683.6	1611.5
		VWN	633.17	388.13	−1338.1	−1058.4	−706.9	1846.7
		VWN-FF	632.59	388.44				
		BP86	661.88	405.03	−1481.3	−1091.5	−751.9	1987.7
		BP86-FF	660.27	406.75				
		HF	710.57		−1173.1	−903.8	−694.2	1635.5
expt			816.62					

[a] Experimental values calculated from the measurement of relative polarizabilities of Knight et al.[14] and the absolute measurement of the atomic polarizability by Molof et al.[17]

in Table 5, the β values and its components show a dramatic increase in magnitude. The values from the MP2 and HF method are closer to each other. It is clear from Table 5 that both VWN and BP86 results are overestimated in comparison with the MP2 and HF values irrespective of the functional and basis set used for the calculation. This is true for both the optimized structures of the hexamer. All the component β values for the hexamer in Table 5 are negative, and the overestimation of the β values is more for the BP86 functional as compared to the VWN. This could be due to the under binding of the electrons by the two DFT functionals. What is clearly noticeable in Table 6 is the sudden drop in the β values for the octamer. This could be due to the compact structure of the octamer which is a result of the magic number of 8-electrons present in its valence shell. All the other calculation including MP2 and HF for both the geometries seems to be completely disordered. We could argue that a small change in geometry can lead to a completely unexpected trend in the β values which are highly sensitive both to the correlation effects as well as structural instability. The MP2 and HF β values are comparable for the TZVP-FIP1 and the Sadlej basis for the PW86 optimized structures of the octamer, whereas the VWN and BP86 β values are comparable for the VWN optimized structures of

Table 6. Static Mean Polarizability, Polarizability Anisotropy, and Mean First-Hyperpolarizability of Na_8 Cluster Optimized with DZVP/A2 (in Atomic Units)

optimized	basis set	method	$\bar{\alpha}$	$\lvert\Delta\alpha\rvert$	β_x	β_y	β_z	β
VWN	TZVP-FIP1	MP2	787.48		−90.6	−2.8	−4.1	90.7
		VWN	706.50	107.28	−44.5	12.2	20.7	50.6
		VWN-FF	705.51	108.68				
		BP86	736.18	109.78	−10.6	51.4	−9.5	53.3
		BP86-FF	734.04	111.15				
		HF	805.62		−29.3	2.7	25.4	38.9
	Sadlej	MP2	804.63		1.6	−7.0	−4.4	8.2
		VWN	711.19	97.8	−35.4	43.0	−17.7	58.4
		VWN-FF	709.65	100.05				
		BP86	744.20	105.40	−55.3	36.6	9.3	67.0
		BP86-FF	741.45	107.79				
		HF	819.90		−39.9	3.8	35.4	53.5
PW86	TZVP-FIP1	MP2	797.96		10.2	−25.7	3.9	27.9
		VWN	715.21	104.11	−43.4	18.8	−15.9	49.9
		VWN-FF	714.22	104.51				
		BP86	743.64	100.91	13.3	18.8	−0.6	23.0
		BP86-FF	741.50	103.94				
		HF	815.15		−10.2	−17.2	−12.6	23.6
	Sadlej	MP2	815.41		10.7	−26.2	3.5	28.5
		VWN	718.60	93.59	−31.2	32.1	122.3	130.2
		VWN-FF	717.14	93.84				
		BP86	750.63	93.55	−76.9	81.5	208.7	236.9
		BP86-FF	747.93	95.69				
		HF	829.78		−13.2	−21.0	−19.1	31.3
Expt.			868.75					

[a] Experimental values calculated from the measurement of relative polarizabilities of Knight et al.[14] and the absolute measurement of the atomic polarizability by Molof et al.[17]

the octamer. There are no experimental β values available for comparison with our values which could have helped to understand the behavior of β values of the sodium clusters better.

Conclusion

We have reported the polarizability and first-hyperpolarizability components for Na clusters and discussed the results obtained using our numerical-analytic approach to the CPKS method in the DFT in comparison to the benchmark ab initio MP2 and HF calculations. The results were compared to experiments wherever possible. First, we find that our numerical-analytic CPKS method gives reasonably good values of static mean dipole polarizabilities. The polarizability results gave the correct qualitative trend comparable with the experiments. The MP2 and HF values of the polarizabilities as well as the first-hyperpolarizabilities were comparable to each other. This is mainly due to the cancellation of errors in the HF method and the basis set effect which even gave HF values in smaller basis closer to the experiment. The MP2 results do not improve the HF values of property although the DFT values seem to converge toward the experimental values as the basis set is increased. Improvement of the functional can lead to faster convergence of results. However, it needs to be kept in mind that the comparison of the polarizabilities from experiments with theory is not as simple, as the temperature effects present in the experiments are missing in the theories used in this paper. It was found that the Sadlej basis gave marginally better values of polarizability than the TZVP-FIP1 basis set as it contains a greater number of polarization functions required for estimation of the response properties. The correlation effects due to the local and nonlocal nature of the exchange-correlation functionals used was discussed for the polarizabilities. However, we were unable to evaluate the precision of our method for the first-hyperpolarizability calculations of the sodium clusters due to the unavailability of experimental values. Measurements of these quantities experimentally, especially for the smaller clusters, would help us get more insight into the response electric properties of the Na clusters. Further the basis set effects and correlation effects due to different exchange-correlation functionals, even meta-GGA for that matter, could be the next step to try. The influence of using different auxiliary basis sets for fitting the coulomb potential, on these properties which we did not attempt in this work, could also be studied. Finally, the advantage due to our single step approximation to the CPKS would only enhance the applicability of the DFT for calculation of the response properties for large systems.

Acknowledgment. K.B.S. acknowledges the financial assistance received from the Council of Scientific and Industrial Research (CSIR) during the course of this work. Financial support from the CONACYT project U48775 is gratefully acknowledged by P.C. This study is, in part, a contribution to a Franco-Mexican collaboration financed through ECOS-Nord Action M02P03.

References

(1) Bonin, K. D.; Kresin, V. V. *Electric-Dipole Polarizabilities of Atoms, Molecules and Clusters*; World Scientific: Singapore, 1997.

(2) Kreibig, U.; Vollmer, M. *Optical Properties of Metal Clusters*; Springer; Berlin, 1995.

(3) Berry, R. S.; Haberland H. In *Clusters of Atoms and Molecules: Theory, Experiment and Clusters of Atoms*; Chem. Phys. 52; Haberland, H., Ed.; Springer-Verlag: Berlin, 1994; p 374.

(4) Alonso, J. A. *Chem. Rev.* **2000**, *100*, 637.

(5) Manninen, M.; Nieminen, R. M.; Puska, M. J. *Phys. Rev. B* **1986**, *33*, 4289.

(6) Moullet, I.; Martins, J. L.; Reuse, F.; Buttet, J. *Phys. Rev. B* **1990**, *42*, 11598.

(7) Moullet, I.; Martins, J. L.; Reuse, F.; Buttet, J. *Phys. Rev. Lett*. **1990**, *65*, 476.

(8) Urban, M.; Sadlej, A. J. *J. Chem. Phys.* **1995**, *103*, 9692.

(9) Solov'yov, I. A.; Solov'yov, A. V.; Greiner, W. *Phys. Rev. A* **2002**, *65*, 053203.

(10) Chandrakumar, K. R. S.; Ghanty, T. K.; Ghosh, S. K. *J. Chem. Phys.* **2004**, *120*, 6487.

(11) Maroulis, G. *J. Chem. Phys.* **2004**, *121*, 10519.

(12) Guan, J.; Casida, M. E.; Köster, A. M.; Salahub, D. R. *Phys. Rev. B* **1995**, *52*, 2184.

(13) Calaminici, P.; Jug, K.; Köster, A. M. *J. Chem. Phys.* **1999**, *111*, 4613.

(14) Knight, W. D.; Clemenger, K.; de Heer, W. A.; Saunders, W. A. *Phys. Rev. B* **1985**, *31*, 2539.

(15) de Heer, W. A. *Rev. Mod. Phys.* **1993**, *65*, 611.

(16) Rayane, D.; Allouche, A. R.; Benichou, E.; Antoine, R.; Aubert-Frecon, M.; Dugourd, Ph.; Broyer, M.; Ristori, C.; Chandezon, F.; Huber, B. A.; Guet, C. *Eur. Phys. J. D* **1999**, *9*, 243.

(17) Molof, R. W.; Miller, T. M.; Schwartz, H. L.; Benderson, B.; Park, J. T. *J. Chem. Phys.* **1974**, *61*, 1816.

(18) Sophy, K. B.; Pal, S. *J. Chem. Phys.* **2003**, *118*, 10861.

(19) Sophy, K. B.; Pal, S. *J. Mol. Struct.: THEOCHEM* **2004**, *676*, 89.

(20) Pal, S.; Sophy, K. B. In *Lecture Series on Computer and Computational Sciences*; Maroulis, G., Simos, T., Eds.; Brill Academic Publishers: The Netherlands; 2005; Vol. 3, p 142.

(21) Parr, R. G.; Yang, W. *Density Functional Theory of Atoms and Molecules*; Oxford University Press: Oxford, 1989.

(22) Dreisler, R. M.; Gross, E. K. U. *Density Functional Theory*; Springer: Berlin, 1990.

(23) Colwell, S. M.; Murray, C. W.; Handy, N. C.; Amos, R. D. *Chem. Phys. Lett.* **1993**, *210*, 261.

(24) Lee, A. M.; Colwell, S. M. *J. Chem. Phys.* **1994**, *101*, 9704.

(25) Kamiya, M.; Sekino, H.; Tsuneda, T.; Hirao, K. *J. Chem. Phys*. **2005**, *122*, 234111.

(26) Jamorski, C.; Casida, M. E.; Salahub, D. R. *J. Chem. Phys*. **1996**, *104*, 5134.

(27) Casida, M. E. In *Recent Developments and Applications of Modern Density Functional Theory*; Seminario, M. J., Ed.; Elsevier: Amsterdam, 1996; p 391.

(28) Ipatov, A.; Fouqueau, A.; del Valle, C. P.; Cordova, F.; Casida, M. E.; Köster, A. M.; Vela, A.; Jamorski, C. J. *J. Mol. Struct.: THEOCHEM* **2006**, *762*, 179.

(29) Guan, J.; Duffy, P.; Carter, J. T.; Chong, D. P.; Casida, K. C.; Casida, M. E.; Wrinn, M. *J. Chem. Phys.* **1993**, *98*, 4753.

(30) Pulay, P. *J. Chem. Phys.* **1983**, *78*, 5043.

(31) Hellmann, H. *Einführung in die Quantenchemie*; Deuticke: Leipzig, 1937; p 285.

(32) Feynman, R. P. *Phys. Rev.* **1939**, *56*, 340.

(33) Köster, A. M.; Calaminici, P.; Flores-Moreno, R.; Geudtner, G.; Goursot, A.; Heine, T.; Ipatov, A.; Janetzko, F.; Martin del Campo, J.; Patchkovskii, S.; Reveles, S. U.; Salahub, D. R.; Vela, A. The deMon Developers: Mexico, 2006.

(34) Kohn, W.; Sham, L. J. *Phys. Rev. A* **1965**, *140*, 1133.

(35) Köster, A. M.; Flores-Moreno, R.; Reveles, J. U. *J. Chem. Phys.* **2004**, *121*, 681.

(36) Dunlap, B. I.; Connolly, J. W. D.; Sabin, J. R. J. *Chem. Phys.* **1979**, *71*, 4993.

(37) Mintmire, W.; Dunlap, B. I. *Phys. Rev. A* **1982**, *25*, 88.

(38) Godbout, N.; Salahub, D. R.; Andzelm, J.; Wimmer, E. *Can. J. Phys.* **1992**, *70*, 560.

(39) Vosko, S. H.; Wilk, L.; Nusair, M. *Can. J. Phys.* **1980**, *58*, 1200.

(40) Perdew, J. P.; Wang, Y. *Phys. Rev. B* **1986**, *33*, 8800.

(41) Perdew, J. P. *Phys. Rev. B* **1986**, *33*, 8822; **1986**, *34*, 7406.

(42) Reveles, J. U.; Köster, A. M. *J. Comput. Chem.* **2004**, *25*, 1109.

(43) Köster, A. M.; Calaminici, P.; Flores, R.; Geudtner, G.; Goursot, A.; Heine, T.; Janetzko, F.; Patchkovskii, S.; Reveles, J. U.; Vela, A.; Salahub, D. R. *deMon2k*; The deMon Developers: Cinvestav, 2004.

(44) Werner, H. -J.; Meyer, W. *Mol. Phys.* **1976**, *31*, 855.

(45) Sadlej, A. J. *Collect. Czech. Chem. Commun.* **1988**, *53*, 1995.

(46) Zeiss, G. D.; Scott, W. R.; Suzuki, N.; Chong, D. P.; Langhoff, S. R. *Mol. Phys*. **1979**, *37*, 1543.

(47) Jaszu'nski, M.; Roos, B. O. *Mol. Phys.* **1984**, *52*, 1209.

(48) Roos, B. O.; Sadlej, A. J. *Chem. Phys*. **1985**, *94*, *43*.

(49) Krack, M. private communication.

(50) Becke, A. D. *Phys. Rev. A* **1988**, *38*, 3098.

(51) Schmidt, M. W.; Baldridge, K. K.; Boatz, J. A.; Elbert, S. T.; Gordon, M. S.; Jensen, J. H.; Koseki, S.; Matsunaga, N.; Nguyen, K. A.; Su, S. J.; Windus, T. L.; Dupius, M.; Montgomery, J. A. *J. Comput. Chem.* **1993**, *14*, 1347.

(52) Martins, J. L.; Buttet, J.; Car, R. *Phys. Rev. B* **1985**, *31*, 1804.

(53) Herzberg, G. *Molecular Spectra and Molecular Structure, I. Spectra of Diatomic Molecules*; Van Nostrand Reinhold: New York, 1950.

(54) Verma, K. K.; Bahns, J. T.; Rajaei-Rizi, A. R.; Stwalley, W. C.; Zemke, W. T. *J. Chem. Phys.* **1983**, *78*, 3599.

(55) Dahlseid, T. A.; Kappes, M. M.; Pople, J. A.; Ratner, M. A. *J. Chem. Phys*. **1992**, *96*, 4924.

CT6003627